

Convective Instability of the Bernstein Wave Propagating Obliquely to the Magnetic Field in Beam-Plasma System

メタデータ	言語: English 出版者: 公開日: 2011-12-20 キーワード (Ja): キーワード (En): 作成者: IDEHARA, Toshitaka, TAKEDA, Mitsuyoshi, ISHIDA, Yoshio メールアドレス: 所属:
URL	http://hdl.handle.net/10098/4666

Convective Instability of the Bernstein Wave Propagating Obliquely to the Magnetic Field in Beam-Plasma System*

Toshitaka IDEHARA,** Mitsuyoshi TAKEDA,** Yoshio ISHIDA**

(Received Apr. 15, 1974)

The Bernstein wave propagating obliquely to the magnetic field is excited by the coaxial probe and is heavily damped by the Landau and/or cyclotron damping with respect to the direction along the field, whose propagation direction may be coincident with that of the maximum value of group velocity ($\partial\omega/\partial\mathbf{k}$). When a rather weak electron beam is injected, the wave is amplified due to the convective instability, whose wave vector \mathbf{k} is determined as follows: the wave number component k_{\parallel} parallel to the field satisfies the Cherenkov excitation condition ($k_{\parallel}v_b \approx \omega$), and then, the component k_{\perp} perpendicular to the field is determined by the dispersion relation $K(\omega, k_{\parallel}, k_{\perp}) = 0$. Increasing the intensity of the electron beam above the threshold value, the spontaneous excitation of the wave is observed, which can be explained consistently as the result of the convective instability of thermal noise in plasma.

1. Introduction

In a warm magnetized plasma, the Bernstein wave has been investigated as one of the interesting waves, because it is the most generalized wave in a high frequency region ($\omega \gtrsim \omega_c, \omega_p$; where ω_c and ω_p are the electron cyclotron and plasma frequencies, respectively). Moreover, from the viewpoint of the wave phenomenon, it has the unique characteristics that it appears as a forward and/or a backward wave with varying the plasma parameters (ω_c, ω_p and electron temperature T_e). The wave is predicted theoretically by Bernstein¹⁾ and its dispersion relation is fully analyzed by Crawford et al.²⁾ in the cases of plasmas with the various velocity distribution function of electrons.

The experimental investigations of the wave are divided into two parts; one of them is the propagation experiment,³⁾ which is concerned with only the wave propagating perpendicularly to the magnetic field, because the wave has not resonant particles and can propagate without Landau or cyclotron damping. The experiment

*Reported in part in Phys. Letters 46A (1974) 409. **Department of Applied Physics.

confirms that the observed dispersion relation is coincident with the theoretical expectation.²⁾ While, the propagation of the wave having the propagation component along the field (hereafter, denoted by 'oblique propagation') has been scarcely investigated experimentally, because of heavy damping of the wave. The other is the experiment of instability of the wave in an electron beam-plasma system,⁴⁾ which is concerned with the oblique propagation satisfying the synchronization condition ($\omega - k_{\parallel} v_{b\parallel} = n\omega_c$). Therefore, the instability experiment has not been supported by the oblique propagation experiment.

In this paper, the characteristics of the oblique propagation of the wave are investigated experimentally, and compared with the calculation of the dispersion relation. Then, when the electron beam is injected, the instability of the wave occurs, because the growth rate of the wave exceeds the damping rate of the wave. These excitation of the wave can be explained by the convective instability.

In the next section, the experimental apparatus and experimental procedures are explained, in §3, the experimental results and discussions are expressed and in final section the conclusion of the paper are described.

2. Experimental Apparatus and Procedures

In order to investigate the propagation of waves and the instability of the wave due to the interaction of an electron beam with a plasma, it is desired that a Maxwellian plasma is produced and an electron beam is injected into this plasma, both parameters of plasma and beam being varied independently. Considering such a requirement, we have set up the apparatus which is consisted of three regions, that is, the dc discharge region, the plasma diffused region (or the beam-plasma system) and the beam generated region, as shown in Fig. 1. Argon gas of the pressure of about $1 \sim 2 \times 10^{-2}$ torr is fed into the discharge region and, by using a method of differential pumping, the gas pressures of the plasma diffused and the beam generated regions are maintained at about $3 \sim 7 \times 10^{-4}$ and $0.8 \sim 1 \times 10^{-4}$ torr, respectively. An external magnetic field is applied along the tube axis and its intensity distribution on axis is shown in Fig. 1. The plasma is produced by a dc discharge and diffused through an orifice (10 mm in diameter and 200 mm in length) and a hole (8mm in diame-

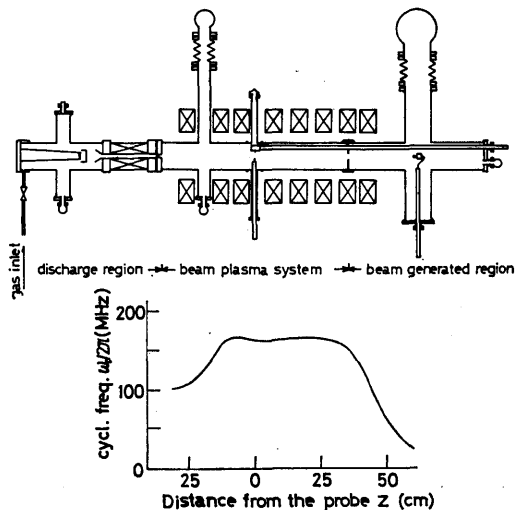


Fig. 1 Experimental apparatus and the distribution of the magnetic field intensity.

ter) at the center of an anode into the plasma diffused region along the external magnetic field. In the region, the field is uniform within 3 percent and its strength is 60 gauss, which is corresponding to $\omega_c/2\pi=168$ MHz. The plasma is supported by the field near the axis of glass tube (95 mm in diameter and 700 mm in length). The plasma density profile in the radial direction is shown in Fig.3. When the discharge current I_d is varied from 2 to 23 mA, the plasma density n_p is varied from 8×10^8 to $9 \times 10^9 \text{ cm}^{-3}$ but the electron temperature is constant at about 6 ~10 eV in the region. The principle of the apparatus is similar to the TP-D machine at the Institute of Plasma Physics, Nagoya University.⁵⁾

An electron beam is produced by the Pierce gun in the beam generated region, and is injected into the plasma diffused region through a hole of 15 mm in diameter. When the acceleration voltage V_b of the beam is changed from 50 to 500 V, the current of the beam I_b changes from 0.18 to 3.1 mA. (The perveance of the gun being about $5 \times 10^{-7} \text{ AV}^{-3/2}$.) The electron density of the beam n_b is varied from 1.5×10^8 to $4.5 \times 10^8 \text{ cm}^{-3}$, but the temperature T_b of the beam is constant at about 0.3 eV.

In order to excite and receive the wave, three coaxial probes are inserted in the plasma diffused region, one of them being movable radially and the other two being movable axially. The signal of the wave excited by a probe is detected using another probe and its propagation pattern is measured and recorded by the interferometer system as shown in Fig.2. The delay line is used in order to determine the direction of the wave propagation. When an intense electron beam is injected and the wave is excited spontaneously, the self correlation is measured by using two of them. From the recorded wave patterns, the wave number and damping rate (or growth rate) are determined. The

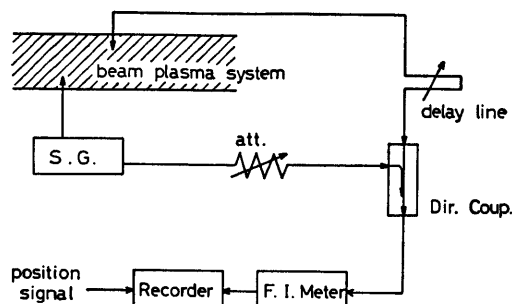


Fig. 2 The interferometer system.

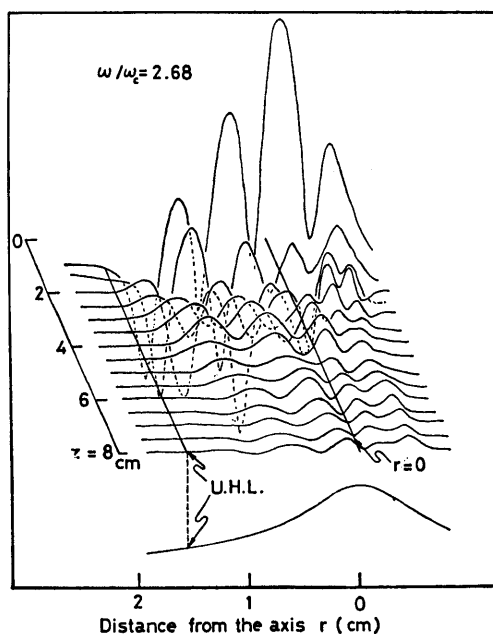


Fig. 3 The propagating wave patterns excited by a coaxial probe and the radial density profile of plasma. The exciting probe is situated at $r=z=0$. U.H.L. shows the upper hybrid layer. $(n_p)_{max}=5.6 \times 10^9 \text{ cm}^{-3}$ ($\omega_p^2/\omega_c^2=16.0$).

excited and/or received frequency is varied from 168 MHz to 500 MHz. When the intensity of received signal is determined, it is compared with and equalized to that of the impulse generator by inserting a known value of attenuation in the transmission line from the plasma to the field intensity meter.

3. Experimental Results and Discussions

3.1 Observation of the wave propagating obliquely to the field

At first, the propagation characteristics of the wave excited by a probe are measured and compared with the calculated dispersion relation. The wave is excited by using one of the z -probes situated on the tube axis (i. e., the center line of the plasma region) and detected by the r -probe situated at the distance of 350 mm from the electron beam inlet. Hereafter, the position of r -probe is defined as the origin of z -axis ($z=0$). The patterns of waves propagating radially are recorded with the separation distance z from the exciting probe (one of z -probes) as a parameter, by using the interferometer system. The result is shown in Fig. 3, with the radial density profile of plasma. This figure may be considered to show the feature of propagation of the wave excited by the probe situated at the point of $z=r=0$. It is seen that the wave does heavily damp along the field (z -direction) but can propagate with little damping across the field (r -direction). Apparently, it propagates obliquely to the magnetic field only in the inner region for the upper hybrid layer ($\omega_p^2 = \omega^2 - \omega_c^2$). The wave damping along the field is very large near the cyclotron harmonics ($\omega = n\omega_c$), where the oblique propagation can not be observed. When only ω/ω_c is nearly equal to a half integer, the damping is comparatively small and the oblique propagation can be observed.

If we plot the points of the same phase on each wave pattern, the wave surfaces are drawn in the r - z plane, which are shown in Fig. 4. The solid and dotted lines show the maximums and minimums of the wave patterns. The wave vector \mathbf{k} must be perpendicular to the wave surface and its direction can be determined by using the delay line in the interferometer system, which is shown by arrows in the figure. In Fig. 4. (a), which corresponds to Fig. 3, the backward property is seen, with respect to both propagation components along and across the field. While, in Fig. 4 (b), the same property is seen with respect to the component across the field but the forward wave property with respect to that along the field. (Here, it is assumed that the group velocity $\partial\omega/\partial\mathbf{k}$, i. e., the energy flow of the wave is directed outward from the exciting probe.) These are very interesting characteristics which is peculiar to the Bernstein wave. In the former case, the absolute instability is expected by the electron beam injection but in the latter case, the convective one is done. In this paper, we are concerned with the latter case, that is, the forward wave property with respect to the propagation component along the field.

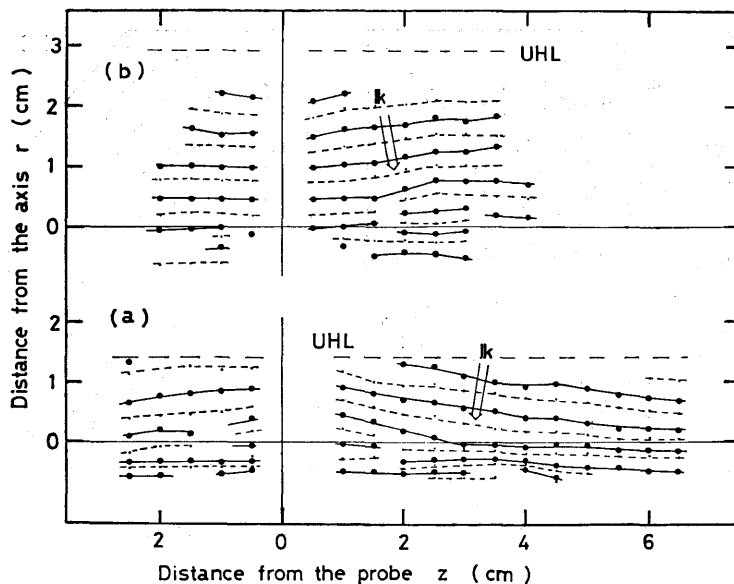


Fig. 4 The Bernstein wave surface. (a) $\omega/\omega_c=2.68$ and $(\omega_p/\omega_c)^2=9$. (b) $\omega/\omega_c=1.55$ and $(\omega_p/\omega_c)^2=6.0$. UHL shows the upper hybrid layer and arrows do the directions of the phase velocities.

3.2 Comparison with the calculated dispersion relation

From the experiment of wave propagation described above, the excited wave is not the standing one but propagates both radially and axially, and the diameter of plasma corresponds to about five or six wavelengths. Therefore, the plasma may be considered to be infinite and uniform for the wave, so that we can analyse the experimental results approximately by using the well-known dispersion relation for the uniform and Maxwellian plasma,

$$K(\omega, k_{\parallel}, k_{\perp}) = 1 + \frac{\omega_p^2}{k^2 v_t^2} \left[1 + \sum_{n=-\infty}^{\infty} \exp(-\lambda) I_n(\lambda) \frac{\omega}{\sqrt{2} k_{\parallel} v_t} Z\left(\frac{\omega - n\omega_c}{\sqrt{2} k_{\parallel} v_t}\right) \right] = 0, \quad \dots\dots(1)$$

where v_t is the thermal velocity of plasma electron, $\lambda = (k_{\perp} v_t / \omega_c)^2$, I_n is the Bessel function of second kind and Z is the plasma dispersion function defined by Fried and Conte.⁶ Under a typical plasma parameter (ω_p/ω_c) , eq. (1) is calculated for real wave vector \mathbf{k} and the complex frequency $\omega + i\omega_i$, which is shown in Fig. 5. From Fig. 5 (a), it is known that both forward ($\partial\omega/\partial k_{\parallel} \cdot k_{\parallel} > 0$) and backward ($\partial\omega/\partial k_{\parallel} \cdot k_{\parallel} < 0$) waves with respect to the propagation component along the field can appear, which explains the experimental results qualitatively. Moreover, it is seen in Fig. 5 (b), that the damping rate (ω_i) increases with k_{\parallel} increased and the increase is larger near the electron cyclotron harmonics because of the cyclotron damping, which

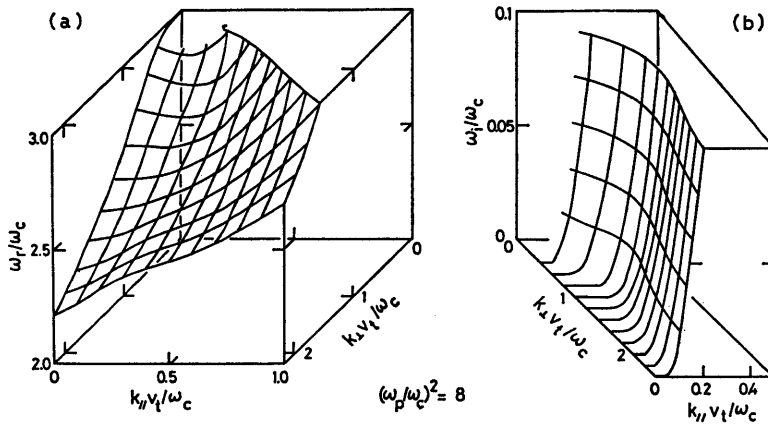


Fig. 5 The dispersion relation surface calculated using eq. (1).
 (a) the frequency ω v. s. wave vectoe \mathbf{k} (b) the
 damping rate ω_i v. s. wave vectork $(\omega_p/\omega_c)^2=8$.

is consistent with the intuitive consideration. The wave can not exist for the large value of k_{\parallel} because of the large damping rate, while it can propagate with little damping, when ω/ω_c is nearly equal to half integer and $k_{\parallel} v_t/\omega_c$ is much smaller than unit, i. e., the condition $|\omega/\omega_c - n| \gg k_{\parallel} v_t/\omega_c$ is satisfied for all integer n . As our experimental condition satisfies the above one, the oblique propagation can be observed.

Under this condition, eq. (1) is rewritten approximately as follows,

$$K(\omega, k_{\parallel}, k_{\perp}) = 1 - \frac{\omega_p^2}{\omega^2} \left[\frac{k_{\perp}^2}{k^2} \sum_{n=1}^{\infty} \frac{\exp(-\lambda) I_0(\lambda) n^2 \omega^2}{(\lambda/2)(\omega^2 - n^2 \omega_c^2)} + \frac{k_{\parallel}^2}{k^2} \exp(-\lambda) I_0(\lambda) \right] = 0. \quad \dots\dots(2)$$

In Fig. 6, are shown the dispersion relation surfaces calculated using eq. (2) for the experimental conditions corresponding to Fig. 4 (a) and (b). Because experimentally determined points (ω, \mathbf{k}) , shown by dark circles in the figure, lies near the

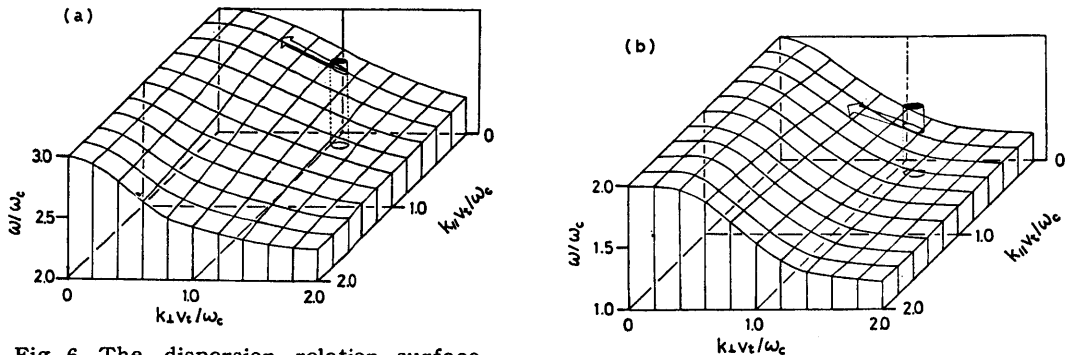


Fig. 6 The dispersion relation surface calculated using eq. (2). (a) $\omega/\omega_c=2.68$ and $(\omega_p/\omega_c)^2=9$.

(b) $\omega/\omega_c=1.55$ and $(\omega_p/\omega_c)^2=6$.

surface, eq. (2) is considered to be good approximation. Arrows show the directions of group velocity of the wave, i. e., the directions of $\partial\omega/\partial\mathbf{k}$. In Fig. 6 (a), it is seen that the wave shows the backward property along the field as well as across the field, while in Fig. 6 (b), the wave is forward with respect to the component along the field, which supports our experimental results shown in Fig. 4 (a) and (b).

3.3 Observation of the amplification of the wave due to the convective instability

The convective instability is expected to occur for the case of forward wave along the field, while the absolute one is done for the backward wave along the field. The former is investigated here and the latter will be reported elsewhere.⁷⁾

Under the experimental condition where the former wave is observed, when an electron beam is injected and its density n_b is increased at constant value of V_b , the damping factor of the wave excited by a probe decreases and then the amplification of wave is observed above the threshold value of n_b , where the convective growth gets over the Landau and/or cyclotron damping. In Fig. 7 (a), the patterns of the propagating waves along the axial direction are shown with the beam current I_b as a parameter. The direction of the phase velocity determined by the delay line is coincident with the direction of electron beam velocity. The amplification factor $k_{\parallel i}$, i. e., the imaginary part of k_{\parallel} , is estimated from the figure and shown in Fig. 7 (b). It is seen that when the beam is not injected and the system is in thermal equilibrium, the excited wave is heavily damped, while with the beam current increased, $k_{\parallel i}$ also increases and becomes positive, so that for an intense electron beam the wave is amplified by the effect of the convective instability.

In Fig. 8 (a) the wave patterns along the axial direction are shown with the beam voltage V_b as a parameter. The wave length λ_{\parallel} is measured from this figure and the phase velocity component $v_{p\parallel}$ ($=\omega\lambda_{\parallel}/2\pi$) is estimated, which is plotted in Fig. 8(b) as a function of V_b . The solid line in the figure shows the electron beam velocity $v_{b\parallel}$ estimated from V_b . Both

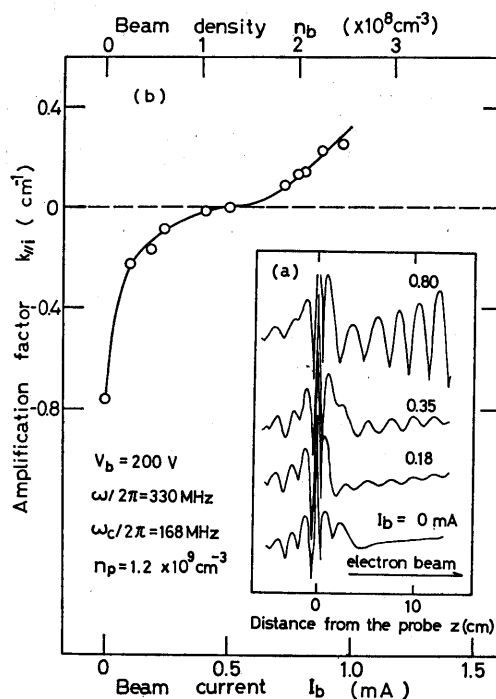


Fig. 7 (a) The wave patterns propagating along the axial direction with the beam current I_b as a parameter. Ar, $p = 7.5 \times 10^{-4}$ torr, $I_d = 4.5$ mA ($n_p = 1.5 \times 10^9$ cm⁻³) and $T_e = 7.8$ eV. (b) The amplification factor $k_{\parallel i}$ as a function of I_b .

the velocity $v_{p\parallel}$ and $v_{b\parallel}$ are almost equal ($v_{p\parallel} \approx v_{b\parallel}$), which verifies that the amplification of the wave is due to Cherenkov type excitation.

The wave patterns propagating along the radial direction are observed with the axial distance z from an exciting probe as a parameter, which is shown in Fig. 9.

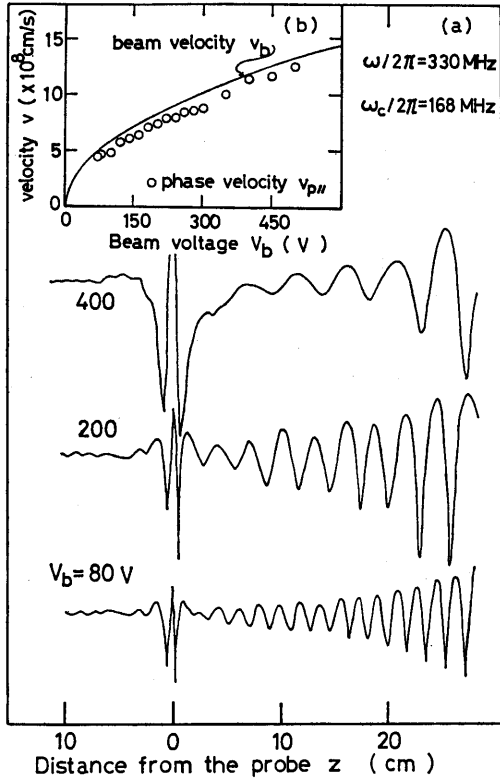


Fig. 8 (a) The wave patterns propagating along the axial direction, with the beam voltage V_b as a parameter. $A_{r,p} = 7.5 \times 10^{-4}$ torr, $n_p = 1.2 \times 10^9 \text{ cm}^{-3}$ and $I_d = 4.6 \text{ mA}$. (b) The phase velocity component $v_{p\parallel} (= \omega/k_{\parallel})$ and the beam velocity $v_{b\parallel}$ as functions of V_b .

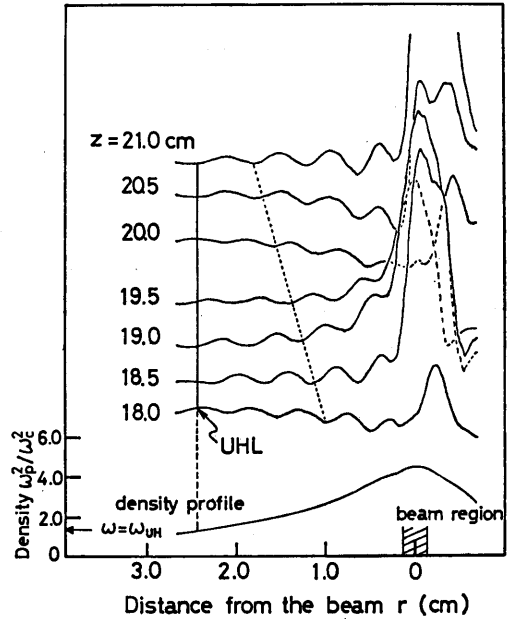


Fig. 9 The wave patterns propagating radially in a beam plasma system as the distance from the exciting antenna z as a parameter and the radial density profile of plasma. A dotted line shows the same phase points of wave and a broken one does the upper hybrid layer (UHL). $V_b = 150 \text{ V}$, $(v_p/\omega_c)^2 = 4.6$ and $\omega/\omega_c = 1.55$.

Plotting the maximums and minimums of these wave patterns on the r - z plane, we can obtain the surfaces of obliquely propagating Bernstein wave as shown in Fig. 10 (a), where the arrow indicates the direction of the phase velocity determined by using the delay line. It shows that the observed wave is confined within the upper hybrid layer, which is consistent with the works of other authors.⁸⁾ Fig. 10 (b) shows the observed wave surfaces with the directions of the phase velocities (denoted by arrows) under the different experimental condition. Considering that the energy source for amplifying the wave is localized at the beam region, the energy flow carried by the wave, i. e., the group velocity of the wave, is considered to be directed

outward from the beam region. Therefore the wave shown in Fig. 10 (a) (where $\omega \ll \omega_{uh}$, ω_{uh} is the upper hybrid frequency) and one of the waves in Fig. 10 (b) (where $\omega \geq \omega_{uh}$) are backward waves and the other in Fig. 10 (b) is a forward wave with respect to the radial direction. This is qualitatively consistent with the theoretical consideration described above.

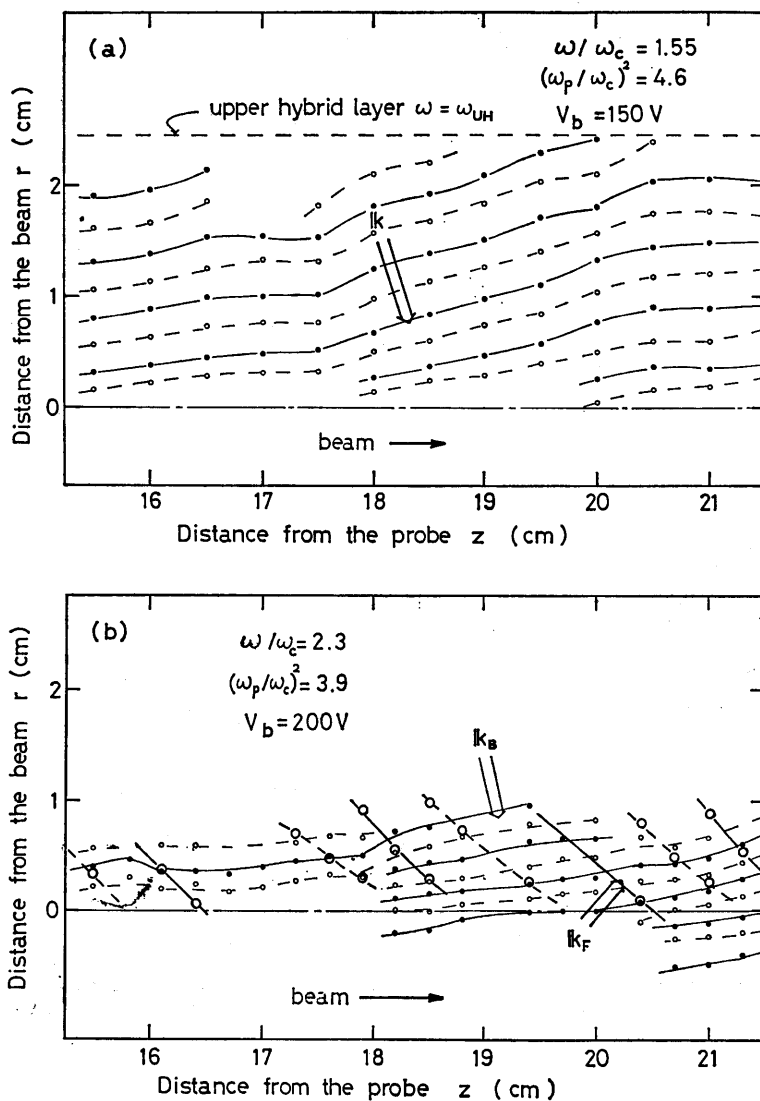


Fig. 10 The surface of the Bernstein wave propagating obliquely. The solid and dotted lines connect the points of the maximums and minimums of the wave patterns. Arrows show the directions of phase velocities v_p . Ar, $p=7.5 \times 10^{-4}$ torr.
 (a) $V_b=150 \text{ V}$, $I_b=1.2 \text{ mA}$, $I_d=8.0 \text{ mA}$, $\omega/2\pi=260 \text{ MHz}$, $\omega/\omega_c=1.55$ and $(\omega_p/\omega_c)^2=4.6$.
 (b) $V_b=200 \text{ V}$, $I_b=1.5 \text{ mA}$, $I_d=4.2 \text{ mA}$, $\omega/2\pi=386 \text{ MHz}$, $\omega/\omega_c=2.3$ and $(\omega_p/\omega_c)^2=3.9$.

In Fig. 11, the relation between the wave number component (k_{\parallel} and k_{\perp}) of the amplifying wave which gives the angle θ of propagation ($\tan \theta = k_{\perp}/k_{\parallel}$), is shown with the plasma density n_p ($\propto \omega_p^2/\omega_c^2$) as a parameter. For rather small density ($\omega_{uh} \lesssim \omega$), two values of k_{\perp} correspond to each value of k_{\parallel} , the smaller one showing the forward wave and the larger one the backward wave with respect to radial direction. However, for large density ($\omega_{uh} \gg \omega$), one value of k_{\perp} corresponds to each value of k_{\parallel} , which shows that only the backward wave exists. The solid and broken lines show the theoretical results calculated using the dispersion relation for infinite plasma described by eq. (2) and eq. (1), respectively, which is good agreement with the experimental results. A little quantitative disagreement may result from the fact that the experimentally observed wave is a cylindrically symmetric wave in a finite system.

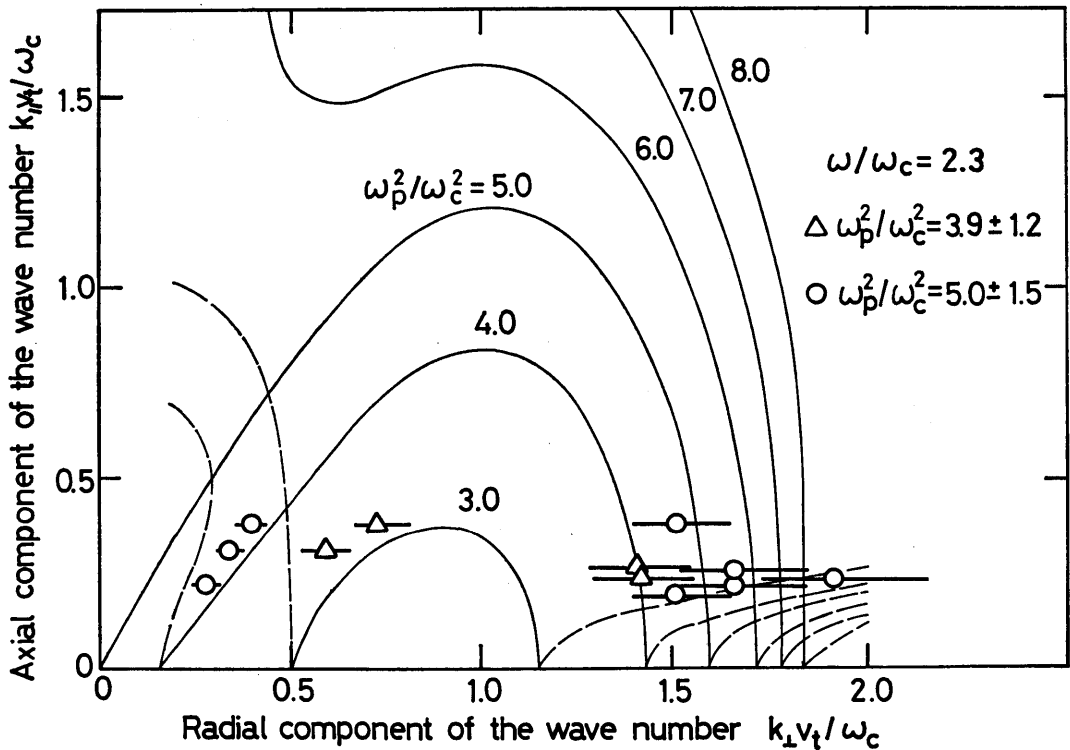


Fig. 11 The relation between the radial and axial components of the wave number. The solid and dotted curves show the calculated ones by using eq. (2) and eq. (1), respectively.

3.4 Spontaneous excitation of the wave due to the convective instability of the thermal noise of plasma.

When the rather weak electron beam is injected, only the externally excited wave is amplified but the spontaneous excitation of the wave is not observed, as described above. However, when a more intense electron beam is injected, the wave is excited

spontaneously, though the external signal is not transmitted.

The curve (a) in Fig. 12 shows the distribution of the excited power along the axis, which sets on at a certain distance from the beam inlet, increases exponentially and saturates finally.

This feature is similar to other experimental results.⁹⁾ The curve (b) in the figure shows the self-correlation of the spontaneously excited wave measured by using the r-probe situated at $z=0$ and one of z-probes movable axially. The direction of phase velocity determined by the delay line coincides with the direction of electron beam velocity and its value $v_{p\parallel}$ calculated from the wavelength λ_{\parallel} ($v_{p\parallel} = \omega\lambda_{\parallel}/2\pi$) is nearly equal to the beam velocity component $v_{b\parallel}$ ($v_{p\parallel} \lesssim v_{b\parallel}$), therefore the excitation mechanism is Cherenkov type.

In Fig. 13, the power distribution of excited wave picked up by r-probe is shown in n_p - ω space with the parameter of beam keeping at constant. Solid curves show the equi-intensity ones and the value of P is that compared with the power of 1 μ V for impedance of 50 Ω .

On the other hand, if we insert one of z-probes at the position denoted by 'EP' in Fig. 12 where the spontaneous excitation does not set on, and excite the wave externally, the wave is amplified by the electron beam before the spontaneous excitation does set on. Using the other of z-probes, the wave signals propagating along an axis are measured and the wave patterns are recorded by the interferometer system. The behavior is shown in Fig. 14 (a) with I_d (or plasma density)

as parameter at the constant frequency and the constant parameters of electron beam. It is seen that the amplification factor $k_{\parallel z}$ varies with I_d but the wavelength remains at constant value which satisfies the Cherenkov excitation condition. The

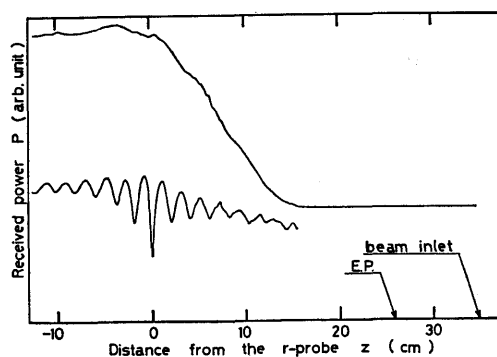


Fig.12 The power distribution of the spontaneously excited wave along the axial direction and self-correlation patterns of the wave. $V_b=210$ V, $I_b=2.75$ mA, $(\omega_p/\omega_c)^2 = 9.5$ and $\omega/\omega_c=2.38$.

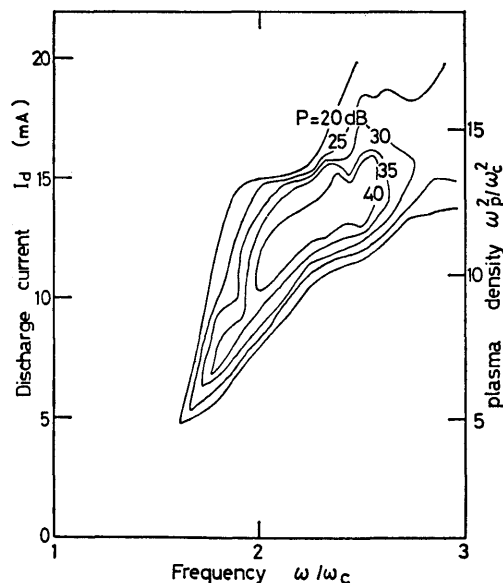


Fig.13 The power distribution of the spontaneously excited wave observed by r-probe. $V_b=145$ V and $I_b=1.5$ mA.

distribution of factor $k_{||z}$ calculated from Fig. 14 (a) and many similar figures is shown in Fig. 14 (b), with the parameter of beam keeping at the same value as Fig. 13. The solid curves show the equi-amplification-factor lines. Comparing the figure with Fig. 13, the region in n_p - ω space where the spontaneous excitation is observed does coincide approximately with that where $k_{||z}$ is larger than $3.0 \times 10^{-2} \text{ cm}^{-1}$. This fact may verify that the spontaneous excitation of the wave is the manifestation of the thermal noise amplified by the convective instability satisfying the Cherenkov excitation condition.

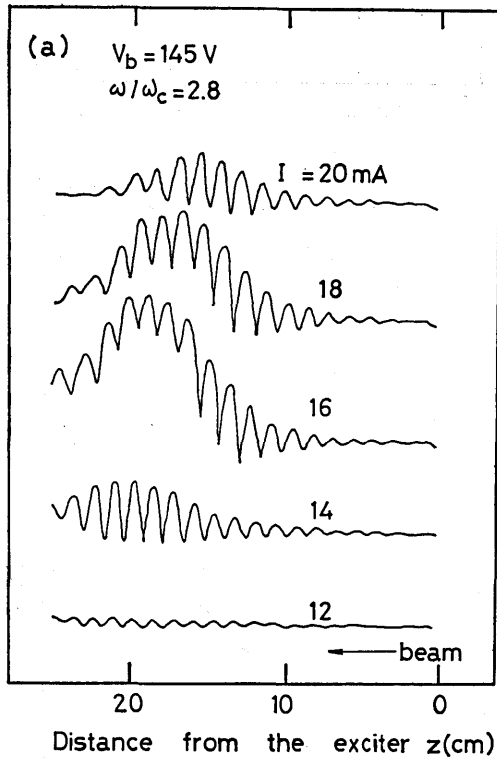
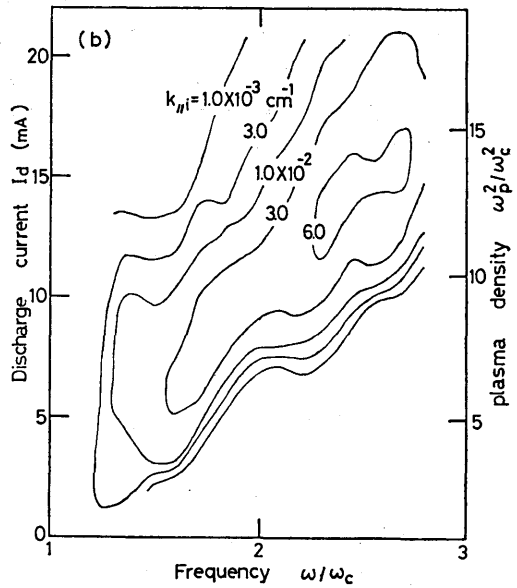


Fig.14 (a) The wave patterns propagating along the axial direction with I_d as a parameter. $V_b=145 \text{ V}$, $I_b=1.5 \text{ mA}$ and $\omega/\omega_c=2.8$.



(b) The distribution of the amplification factor $k_{||z}$ calculated from the propagating wave patterns. $V_b=145 \text{ V}$ and $I_b= 1.5 \text{ mA}$.

4. Conclusion

In order to investigate the mechanism of an instability of Bernstein wave in a beam-plasma system, the comparison with the study of the wave propagation must be done. The propagation of the wave in a Maxwellian plasma is studied in detail and then, the instability in a plasma penetrated by an electron beam is done for various plasma and beam parameters. The results can be described in brief as follows.

- i) In a Maxwellian plasma, the Bernstein wave excited by a coaxial probe can

propagate obliquely to the magnetic field at the frequency far from the cyclotron harmonics ($|\omega - n\omega_c| \gg k_{\parallel} v_t$) but can do only perpendicularly to the field near the cyclotron harmonics because of heavy Landau and/or cyclotron damping along the field.

ii) The measurement of the propagating wave surface shows that with respect to the propagation component along the field, the forward and/or backward waves can exist, and the observed results can be explained consistently by the calculated one for an infinite and uniform plasma, because the diameter of plasma is much larger than the radial wavelength.

iii) In the case where the forward wave exists, the amplification of the externally excited wave due to the convective instability is observed when a rather weak electron beam is injected. The wave number component k_{\parallel} satisfies the Cherenkov excitation condition and the component k_{\perp} is determined from the dispersion relation $K(\omega, k_{\parallel}, k_{\perp}) = 0$.

iv) When a more intense electron beam is injected, the spontaneous excitation of the wave is observed. From comparison of the power distribution of excited waves with the distribution of the amplification factor k_{\parallel} in $n_p - \omega$ space, the excited wave can be considered to be the manifestation of the thermal noise in plasma amplified by the convective instability satisfying the Cherenkov excitation condition.

When the backward wave exists, the absolute instability is expected to occur by injecting an electron beam.¹⁰⁾ This instability is under study and will be reported elsewhere in the near future.

Acknowledgements

The authors wish to express their sincere thanks to Professor S. Tanaka, Kyoto University for his encouragement and valuable discussions. They also thanks to Mr. N. Miyama for his assistance on the experiment. This work was partially supported by a Grant in Aid from the Ministry of Education in Japan.

References

- 1) I. B. Bernstein ; Phys. Rev. 109 (1958) 10.
- 2) J. A. Tataronis and F. W. Crawford ; J. Plasma Phys. 4 (1970) 231, and 4 (1970) 249.
- 3) S. Gruber and G. Bekefi; Phys. of Fluids 11 (1968) 122.
F. Leuterer ; Plasma Phys. 11 (1969) 615.
- 4) M. Seidl and P. Sunka; Nucl. Fusion 7 (1967) 237.
B. R. Kusse and A. Bers; Phys. of Fluids 13 (1970) 2372.
T. Idehara, K. Ohkubo and S. Tanaka; J. Phys. Soc. Japan 27 (1969) 187.
- 5) K. Takayama, M. Ohtsuka, Y. Tanaka, K. Ishii and Y. Kubota; in Proceedings of the Seventh International Conference on Phenomena in Ionized Gases (Gradevinska, Knjiga, Beograde, Yugoslavia, 1966) vol. I p. 420
- 6) B. D. Fried and S. D. Conte; The Plasma Dispersion Function (Academic Press, New

York, 1961).

- 7) T. Idehara, M. Takeda, N. Miyama and Y. Ishida; to be published.
- 8) S. Hiroe and H. Ikegami ; J. Phys. Soc. Japan 34 (1973) 522.
- 9) T. Idehara, K. Ohkubo and S. Tanaka ; J. Phys. Soc. Japan 30 (1971) 1169.
K. Mizuno and S. Tanaka; Phys. Rev. Letters 29 (1972) 45, and J. Phys. Soc. Japan 35 (1973) 1753.